Nat Hazards (2009) 48:275–294
DOI 10.1007/s11069-008-9264-0

ORIGINAL PAPER

Urban social vulnerability assessment with physical proxies and spatial metrics derived from air- and spaceborne imagery and GIS data

Annemarie Ebert · Norman Kerle · Alfred Stein

Received: 16 November 2007 / Accepted: 6 June 2008 / Published online: 1 July 2008

Abstract Risk management in urban planning is of increasing importance to mitigate the growing amount of damage and the increasing number of casualties caused by natural disasters. Risk assessment to support management requires knowledge about present and future hazards, elements at risk and different types of vulnerability. This article deals with the assessment of social vulnerability (SV). In the past this has frequently been neglected due to lack of data and assessment difficulties. Existing approaches for SV assessment, primarily based on community-based methods or on census data, have limited efficiency and transferability. In this article a new method based on contextual analysis of image and GIS data is presented. An approach based on proxy variables that were derived from high-resolution optical and laser scanning data was applied, in combination with elevation information and existing hazard data. Object-oriented image analysis was applied for the definition and estimation of those variables, focusing on SV indicators with physical characteristics. A reference Social Vulnerability Index (SVI) was created from census data available for the study area on a neighbourhood level and tested for parts of Tegucigalpa, Honduras. For the evaluation of the proxy-variables, a stepwise regression model to select the best explanatory variables for changes in the SVI was applied. Eight out of 47 variables explained almost 60% of the variance, whereby the slope position and the proportion of built-up area in a neighbourhood were found to be the most valuable proxies. This work shows that contextual segmentation-based analysis of geospatial data can substantially aid in SV assessment and, when combined with field-based information, leads to optimization in terms of assessment frequency and cost.

A. Ebert (✉)
UFZ, Helmholtz Centre for Environmental Research—UFZ, Permoserstr. 15, 04318 Leipzig, Germany
e-mail: annemarie.ebert@ufz.de

N. Kerle · A. Stein
International Institute of Geo-information Science and Earth Observation (ITC), Hengelosestraat 99, P.O. Box 6, 7500 AA Enschede, The Netherlands
e-mail: kerle@itc.nl

A. Stein
e-mail: stein@itc.nl

Keywords Social vulnerability assessment · Object-oriented image analysis · Proxy variables · Tegucigalpa

Abbreviations

DSM	Digital surface model
nDSM	Normalized digital surface model
DTM	Digital terrain model
GIS	Geoinformation System
OOA	Object-oriented analysis
PV	Physical vulnerability
SV	Social vulnerability
SVI	Social Vulnerability Index
TTA	Test and training areas

1 Introduction

In recent decades the number of natural disasters has been increasing, affecting a growing number of people by causing extensive loss of life and property damage. Every populated place faces a certain risk to be affected by a disaster, the size of which depends on location-specific (i) hazards present, (ii) vulnerability and (iii) the number of elements at risk (Fig. 1). This relation can be expressed as:

$$\text{Risk} = \text{f}(\text{hazard, vulnerability, elements at risk}) \tag{1}$$

Disaster management tools are available to help minimize the risk and thereby the impact of a hazardous event (Fig. 1) but require detailed knowledge about the risk a particular area is facing.

Risk analysis encompasses the assessment of all factors shown in Eq. 1. The hazard, i.e. the probability of a potentially damaging event with a certain magnitude to occur (Cardona 2003), can be expressed in absolute values, as can the number of elements at risk. Methods to evaluate these physical concepts have been shown in previous studies (Bacon et al.

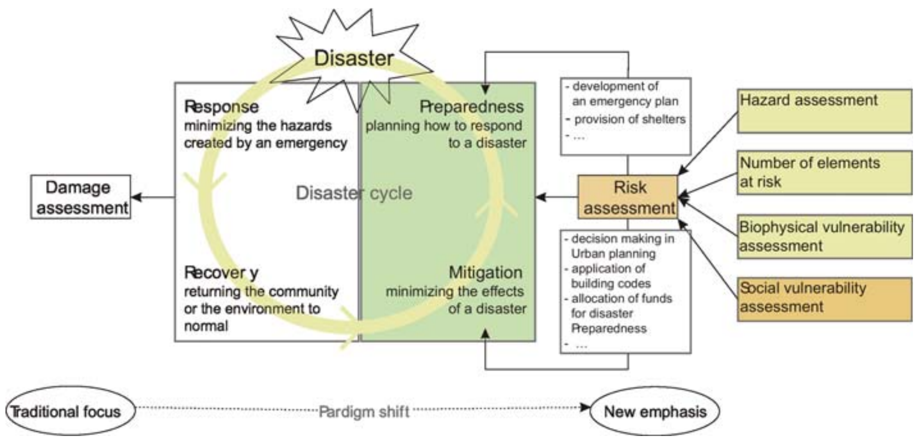

Fig. 1 Disaster management cycle with the position of social vulnerability assessment

1997; Giardino et al. 2005; van Westen et al. 2005). Vulnerability, on the other hand, is more multi-faceted. In addition to the social and physical sides, also environmental and economic aspects can be considered, resulting in a variety of research perspectives and term definitions. Rashed and Weeks (2003a) see vulnerability as an ill-posed problem defined by multiple solutions and uncertainty about the concepts, rules and principles involved to reach these solutions. Physical vulnerability (PV) refers to the properties of physical structures that determine their potential damage in case of a disaster (e.g. material type and construction quality). Theoretical rules and considerations exist for its assessment, although a comprehensive assessment is challenging as a detailed database is required (O'Hare and Rivas 2005). Due to the sound conceptual basis, given adequate data availability, PV is relatively straightforwardly assessed and frequently used synonymously with vulnerability in general. This results in implicit neglection of SV, which refers to the socio-economic circumstances and individual characteristics that make people susceptible to the impact of a hazardous event (Cutter et al. 2003). In this study the approach by Clark et al. (1998) is applied, defining SV as "people's differential incapacity to deal with hazards, based on the position of the groups and individuals within both the physical and social worlds", which has to be assessed with respect to the particular hazard or combination thereof (e.g. floods and/or landslides; Coburn et al. 1994). Rashed and Weeks (2003b) further discussed that vulnerability can have different sources. It can either be inherent, e.g. due to the affiliation to a certain marginalized group (persistent vulnerability), or result from a choice, e.g. people choosing to live in a hazard-prone environment (situational vulnerability). This can also be seen as the difference between 'who you are' and 'where you are', respectively (Rashed and Weeks 2003a).

Emdad Haque and Etkin (2007) point out the significance of societal dimensions in hazard analysis, and thereby in risk analysis. At the moment, SV still lacks a broadly accepted definition, though several examples for its assessment exist (Briguglio 2003; Haki et al. 2004), based on indices derived from the analysis of census data (Cutter et al. 2003; Dwyer et al. 2004) or from data collected using community-based methods (Flint and Luloff 2005; Allen 2006). Census data, however, are collected for a different purpose and consequently neglect important information about hazard perception and mitigation abilities. Moreover, they are, if at all, only available on neighbourhood level or coarser, and with a temporal resolution of no more than 5–10 years. Community-based surveys on the other hand are very detailed but also time-consuming and lead to results that can be subjective and are difficult to up-scale (Birkmann 2005; Villagrán de León 2006). Both traditional approaches used for SV assessment thus can provide important information yet have limited efficiency and/or transferability. Additionally, the generally low temporal resolution of censuses and of community-based surveys that go beyond very local multi-temporal studies are poorly suited to capture the dynamic character of SV in an operational manner.

This work builds on recent studies that have identified physical expressions of SV. For example, Wu et al. (2002) analysed housing structures and the built environment in a GIS-based study of SV, similar to Clark et al. (1998) who also studied the link to land use and transportation infrastructure and Rashed and Weeks (2003b) who considered the physical and social conditions to be intricately linked, making the former indicative of the latter.

The objective of this work was to test the utility of lidar, optical satellite and GIS data to derive SV-relevant information by using physical proxy variables to describe not-directly observable phenomena, with better time and cost efficiency and higher temporal resolution compared to the traditional analysis methods. Proxies are measurable variables that can provide insight into phenomena that cannot be directly observed or measured, but which are conceptually linked.

Physical expressions of social vulnerability (SV), such as settlement type or vegetation density, can be best expressed in terms of spectral, geometric and topological characteristics of land cover elements forming complex urban units. Therefore, the proxies in our study were addressed in a framework of contextual object-oriented analysis (OOA), which to our knowledge has not been employed before in SV research. Additionally, the focus is laid on Honduras, a less developed country where spatial and physical factors of SV are even more pronounced (Rashed and Weeks 2003b), where current census data as used by Cutter et al. (2003), Clark et al. (1998) and Wu et al. (2002) are often not available, and where disaster casualty figures show vulnerability to be the highest.

2 Study area

The test area for this study contained 87 neighbourhoods (in total ca. 3 × 3 km) in Tegucigalpa, the capital city of Honduras. Tegucigalpa is located at about 14° N and 87° W in the highlands of central Honduras at an elevation of approximately 1,000 m asl (Fig. 2).

With 53.0% of the population living below the national poverty line (UNDP 2005), Honduras is a country with medium development (UNDP 2005) and limited industrial and commercial infrastructure. Tegucigalpa today has more than one million inhabitants and is growing steadily (on average about 2.8% p.a. from 1988 to 2001) in an unplanned manner, also into hazard-prone terrain, such as steep slopes surrounding the city and along the rivers, often the only available and affordable spaces for building construction (Angel et al. 2004). The proximity to the labour market and urban facilities is for most migrants more important than living in a safe environment, a known worldwide phenomenon (O'Hare and Rivas 2005).

Ecological and land use changes, e.g. by deforestation of slopes, straightening of rivers and loss of natural flooding areas, also result from city growth, which in turn increase the

Fig. 2 Location of the study area Tegucigalpa in Honduras

city's vulnerability (Davidson 2006). This became apparent during Hurricane Mitch that struck Tegucigalpa in 1998 and triggered numerous landslides on deforested slopes and severe flooding, which caused thousands of fatalities and destroyed large parts of the city's infrastructure, that were located in hazard-prone areas (CINDI 1998).

3 Geoinformatics in disaster management

The utility of geoinformatics tools for all aspects of disaster management has been amply illustrated in the literature. In particular remote sensing technologies have been used for (i) predisaster applications, such as scenario modelling (Iverson et al. 1998; Tralli et al. 2005), (ii) forecasting of events (e.g. of volcanic eruptions or windstorms), (iii) early warning and event monitoring (Ramsey and Flynn 2004) and (iv) damage assessment and monitoring of land use changes after a disaster (Kerle 2002; Arciniegas et al. 2007).

Progress is also being made in the use of remote sensing data in quantitative risk researches, e.g. for hazard analysis (Lee et al. 2004), assessment of urban vulnerability including SV (Rashed and Weeks 2003a), or vulnerability of buildings (Müller et al. 2006). So far, most studies are limited to the description of one or few components of risk (Eq. 1) or provide a comprehensive assessment of only the factors that can be directly measured (van Westen et al. 2005).

The main limitations in the application of geoinformatics in comprehensive risk management are (i) the high data demand and cost, (ii) the need for an integrated analysis of multi-type/format data, (iii) the need for frequent risk assessments and database updating due to rapid urbanization and (iv) that information also about concepts that are difficult to map directly, such as SV, has to be included. However, the field is also benefiting from developments in other remote sensing areas, such as automatic mapping and classification of buildings with InSAR (Balz and Haala 2003; Stilla et al. 2003), laser data (Dash et al. 2004), or Ikonos imagery (Fraser et al. 2002). Rashed and Weeks (2003b) focused the assessment of vulnerability of urban places (urban vulnerability) using pixel-based spatial metrics and a spectral unmixing approach. Our study focuses on the assessment of SV based on multi-source remote sensing and GIS data, using contextual information and multi-scale interpretation implemented in OOA. Contextual information provides knowledge about distances (e.g. to hazard zones) and the local environment (e.g. slope) of a building, while multi-scale analysis considers different spatial dimensions, ranging from sub-building features to entire city districts. The resulting delineation and application of proxy variables, as explained in Sect. 4, support the identification of parameters that are non-physical and not directly visible, hence which cannot be assessed from satellite data using alternative methodologies, such as pixel-based analysis.

4 Methodology

4.1 The advantages of OOA for vulnerability analysis

Image classification has traditionally been done using pixel-based analysis, where each pixel is classified based on its spectral characteristics and without contextual information. More recently developed OOA methods aim at imitating human cognition and begin with segmentation of image data on different spatial scales that depend on the desired level of generalization, the spatial resolution of the image, as well as the inherent scale of the objects.

For example, chimneys can be preserved as individual objects in one level, while in another level entire buildings constitute the smallest spatial unit. The result of the segmentation process is an image hierarchy that contains different levels with objects of different sizes, where each object knows all properties of its sub-, super- and neighbour-objects (Baatz et al. 2004). All of those, together with the objects' geometric and spectral characteristics, can then be incorporated in the interpretation of the resulting image segments at only one or at several segmentation levels (Blaschke and Strobl 2001; Baatz et al. 2004). Small spectral inhomogeneities that normally lead to wrongly classified pixels are averaged out during the segmentation, allowing increased classification accuracies. However, previous studies also showed that segmentation alone does not improve the classification result, but rather that a proper integration of semantic information is needed in the post-segmentation analysis (Gao et al. 2007). In the context of risk, this is critical as the position and spatial arrangement of image objects in their natural and man-made environment strongly determine the SV (Clark et al. 1998; Wu et al. 2002; Rashed and Weeks 2003b).

Object properties in this study comprise spectral and textural information, as well as shape characteristics, object size and distance to all other image objects, which were analysed in Definiens. Beneficial is that both image data and auxiliary raster and vector data types, such as elevation models, thematic layers or other GIS data, can be included in image segmentation and classification. This allows class descriptions that support a detailed land cover and land use assessment by providing a rich contextual analysis framework. Specific classes, such as buildings within a hazard zone or buildings on steep slopes, can be identified directly (Sect. 4.6). Also GIS data can be directly used as a basis for class descriptions, as was done here with polygon outlines of a cemetery and rivers. The combination of spectral features with shape characteristics and auxiliary data yields classes that are suitable for a comprehensive assessment of living environments, and which in turn are indicators for the assessment of SV. These indicators are then expressed using object-based proxy variables that have previously been used in PV assessment, e.g. building heights for flood vulnerability, but to our knowledge not in a SV context. Figure 3 presents the methodology of this study, while Table 1 gives an overview of the data used.

4.2 Data pre-processing

The panchromatic and multi-spectral Quickbird images acquired simultaneously were merged using wavelet transformation (Hirschmugl et al. 2005), while the RecourseSat-1 (IRS-P6) image remained unaltered. The lidar-derived digital surface model (DSM) available for a part of the study area was used to extract a digital terrain model (DTM), employing the local point cloud segmentation procedure described in Vosselman et al. (2004). The difference between the DSM and the DTM in turn provided absolute heights of all objects situated on the ground surface, such as houses and trees. Points from the lower resolution DTM vector set available for the entire city were interpolated using triangulation and the slopes calculated. Additional information from thematic city maps was digitized where relevant (e.g. building use and distribution of service infrastructure). All available GIS data (Table 1) were matched and brought to the same reference system.

4.3 Segmentation of the Quickbird image

Unlike the DTM, the normalized DSM (nDSM, Sect. 4.2) that contains absolute heights of all objects on the surface was only available for a small part of the study area. Thus

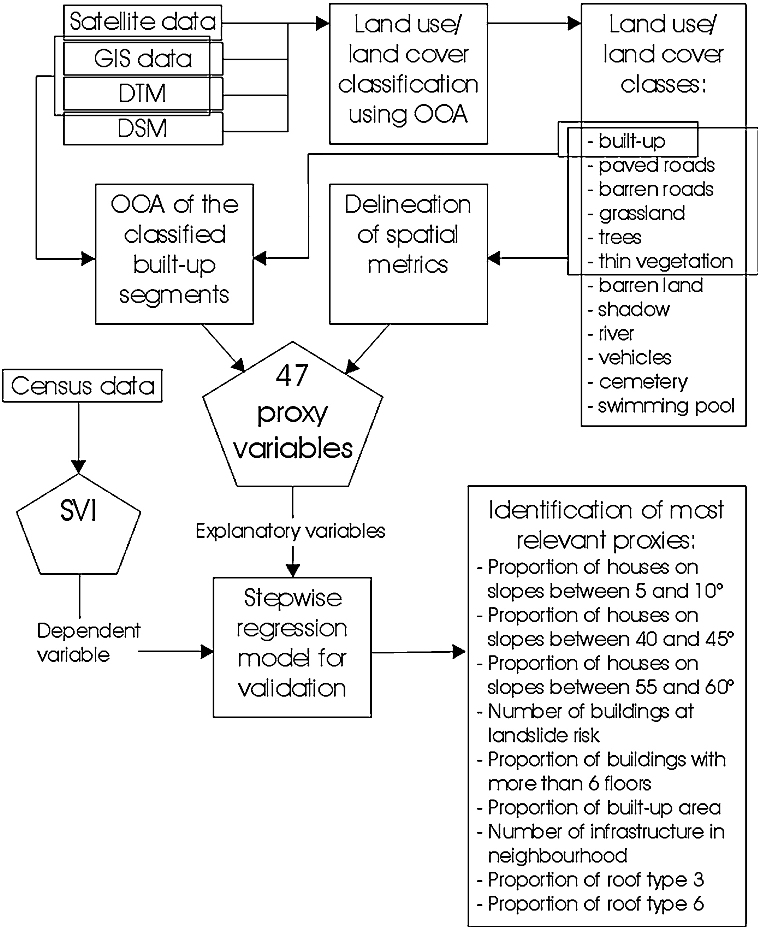

Fig. 3 Main steps of the analysis and most relevant results

the image analysis was performed both with and without the nDSM (Project 1 and Project 2, respectively), with image segmentation in both cases also incorporating the pansharpened Quickbird image and the digitized outlines of the cemetery and the rivers. Different segmentation parameters were applied to create three image levels for the classification of the Quickbird image only and four for the classification of the Quickbird image in combination with the nDSM (Table 2). The additional level here was used to distinguish flat and built-up areas based on data from the nDSM. The segmentation parameters were found based on trial-and-error and evaluated by visual analysis. Even though Project 2 was just a subset of the first, new segmentation parameters had to be found to ensure suitable segment borders also reflecting the additional nDSM data, such as building outlines. The lack of a methodology for finding objective parameters and evaluation tools other than visual analysis is a known limitation of Definiens, or indeed segmentation-based analysis in general, although several groups are working on ways to overcome this limitation (e.g. Espindola et al. 2006; Zhang and Maxwell 2006).

Table 1 Raster and vector data used for this study in Tegucigalpa

Type	Source	Date	Format	Resolution
Quickbird	Digital Globe	12/2000	Raster	ms[e]: 2.4 m; pan[f]: 0.61 m
ResourceSat P-6	NRSA[b]	04/2006	Raster	5.8 m
DTM[a] (based on point data)	PMDN[c]	n.a.	Vector	1.5 m
Gridded Lidar DSM	USGS[d]	03/2000	Raster	1 m
Hazard maps (floods and landslides)	USGS	2002	Vector	1:10,000
Hurricane Mitch damage maps (flood and landslide outlines)	USGS	2002	Vector	1:10,000
Main river network	Princeton University	2000	Vector	1:10,000
Various infrastructure (from maps)	n.a.	2002 and 2004	Vector	n.a.

[a] DTM: digital terrain model

[b] NRSA: National Remote Sensing Agency

[c] PMDN: Proyecto de Mitigación de Desastres Naturales

[d] USGS: United States Geological Survey

[e] ms: multi-spectral

[f] pan: panchromatic

Table 2 Segmentation parameters and extracted land use/land cover classes for the analysis of the pan-sharpened Quickbird image only (upper part) and in combination with the nDSM (lower part)

IL	Classes	SP	Col.	Comp.
OOA of the pansharpened Quickbird image				
1	Barren land, barren road, built-up, grassland, graves, paved roads, river, shadow, swimming pools, thin vegetation, trees	30	0.7	0.9
2	Trees, vehicles, graves	30	0.7	0.9
3	Barren land, barren road, paved roads, shadow, built-up area (7 roof types), swimming pools, grassland (dry, medium, healthy), thin vegetation	45	0.7	0.9
OOA of the pansharpened Quickbird image in combination with the nDSM				
1	Flat, high	30	0.7	0.9
2	Barren land, built-up, grassland, paved roads, river, shadow, swimming pools, trees, thin vegetation	30	0.7	0.9
3	Trees, vehicles	30	0.7	0.9
4	Barren land, paved roads, shadow, built-up area (7 heights), swimming pools, grassland (dry, medium, healthy), thin vegetation	50	0.7	0.9

Image levels 1 and 2, respectively, contain the final classification result

Abbreviations: IL, image level; SP, scale parameter; Col., colour criterion; Com., compactness

4.4 Classification of the Quickbird image

Twelve main land use/land cover classes were initially classified from the data set (Fig. 3). For the assessment of SV, the most relevant classes are built-up areas (buildings) and roads as the principal indicator for habitation, and vegetation for a characterization of the neighbourhood (Ridd 1995; Rashed and Weeks 2003b). Class descriptions were done using representative samples from the study area (test and training areas, TTA) and by creating knowledge-based fuzzy sets. Fuzzy sets refer to the object properties (features), such as spectral values, shape characteristics, relations to other image objects, or information from thematic layers (such as elevation data). They determine a range of values for a certain feature that is characteristic for the respective class and are expressed mathematically in membership functions (Baatz et al. 2004). A main aspect of Project 1 was the distinction of different roof materials as a principal descriptor of housing types, based on spectral information, while Project 2 yielded a classification of buildings based on their height. Seven different roof types were distinguished in the study area, although additional ground truth information or better multi-/hyperspectral data would be necessary to determine the actual material of the roof types. Since neither was available for this study, it was only tested if roof material in principle can serve as a proxy for SV (see Sect. 4.6). Different vegetation types were distinguished using NDVI values, texture measures and visual interpretation (Myint 2007). Finally, two main road qualities (paved and barren), critical indicators of urban living conditions, were identified based on spectral properties. The overall classification accuracy, calculated using independent TTAs, was 84.3% for the image without the nDSM, and 89.1% for the image with the nDSM. Thus, elevation information is a valuable contribution for the extraction of building footprints and for certain class descriptions, e.g. for the separation between paved roads and spectrally similar roof types.

4.5 Texture analysis of the Quickbird and IRS-P6 image

Image texture describes the distribution of grey values in an image and thus characterizes the homogeneity of settlements, and can be calculated in different ways, e.g. using measures such as homogeneity, variance and skewness (Tuceryan and Jain 1998; Herold et al. 2003). The homogeneity of the Quickbird image was calculated using a Grey Level Co-occurrence Matrix (GLCM) in Definiens, which is based on the frequency of specific pixel combinations in the image (Baatz et al. 2004). Variance and skewness were calculated in Erdas Imagine for the Resource-Sat image (see Table 3).

4.6 Delineation of proxy variables

Proxy variables can be statistical census data, grey values of single pixels (e.g. Lawrence et al. 2002), or data related to diverse object characteristics. They are frequently used in disaster research where the parameter of interest cannot be directly assessed. Cutter et al. (2003) identified a total of 17 measures, such as age, gender or socio-economic status to characterize SV. Similarly, Rashed and Weeks (2003b) used vegetation ratios as a proxy for wealth of a neighbourhood, while Wu et al. (2002) considered land use to be a general proxy of a place's exposure to flood hazard. Given our focus on image-derived information, the following indicators were found to be relevant for SV assessment and are expected to have physical expressions:

- Socio-economic status
- Commercial and industrial development
- Service infrastructure/lifelines, and distance to those.

Table 3 shows how the original indicators for SV assessment were translated into proxy variables that can be primarily delineated from remote sensing data. It was found that the socio-economic status of a household in Tegucigalpa can best be

Table 3 Criteria for the assessment of SV with spatial expression and explanation of the delineated proxy variable

Original indicator	Parent proxy	Supporting proxy	
Socio-economic status	Settlement type	Proportion of built-up and vegetated area (4 proxies)	Proportion of area per administrative neighbourhood covered with buildings only, buildings and roads, vegetation, and barren land (after Ridd 1995)
		Road conditions (1)	Proportion of paved road of all roads in the neighbourhood
		Roof type (7)	Seven spectrally different roof materials
		Available infrastructure (1)	Amount of infrastructure per neighbourhood
		Texture (10)	For IRSP-6 image: mean of variance and skewness, standard deviation of variance and skewness for 3 × 3 pixel window;
			For Quickbird image: mean of variance and skewness for 3 × 3 pixel window, mean and standard deviation of homogeneity in 45° direction
	Topographic location	Slope position (12)	12 slope classes in 5° intervals
		Proportion of buildings in hazard zone (2)	Proportion of buildings in landslide hazard zone and flood hazard zone based on all buildings in the neighbourhood
Commercial and industrial development	Commercial development	Building heights (7)	1-, 2-, 3-, 4-, 5-, 6- and more than 6-storey buildings
Distance to lifelines	Distance to lifelines	Distance measures (3)	Distance of each building to next infrastructure (0–100, 100–250, >250 m)

The detailed number of proxies is given in parentheses

described via the settlement type where it is located, and by its topographic location. Areas with only little vegetation and poor road quality, little economic and infrastructural development and/or situated in hazard-prone areas such as steep slopes were considered to have the lowest coping capacities and thus to be most socially vulnerable. Tegucigalpa, similar to other Central American capital cities, also has more luxurious neighbourhoods located in areas with steeper slopes, for reasons more related to the view, seclusion or better environmental characteristics such as air quality. This generally results in higher situational and lower persistent vulnerability. Such areas can still be identified based on spatial metrics related to building patterns and surfaced road and vegetation ratios.

To describe the settlement type, the proportion of built-up and vegetated area was calculated for each neighbourhood of the city (see outlines in Fig. 4). Proportion measures are spatial metrics originating from ecology that characterize and compare settlement areas, allowing spatial variations and temporal changes in the urban morphology to be quantified (Herold et al. 2003; Rashed and Weeks 2003b; Herold and Clarke 2007). This study was devised as a monotemporal assessment; thus, the calculation of spatial metrics focused on proportion measures to characterize neighbourhoods. For example, roads were

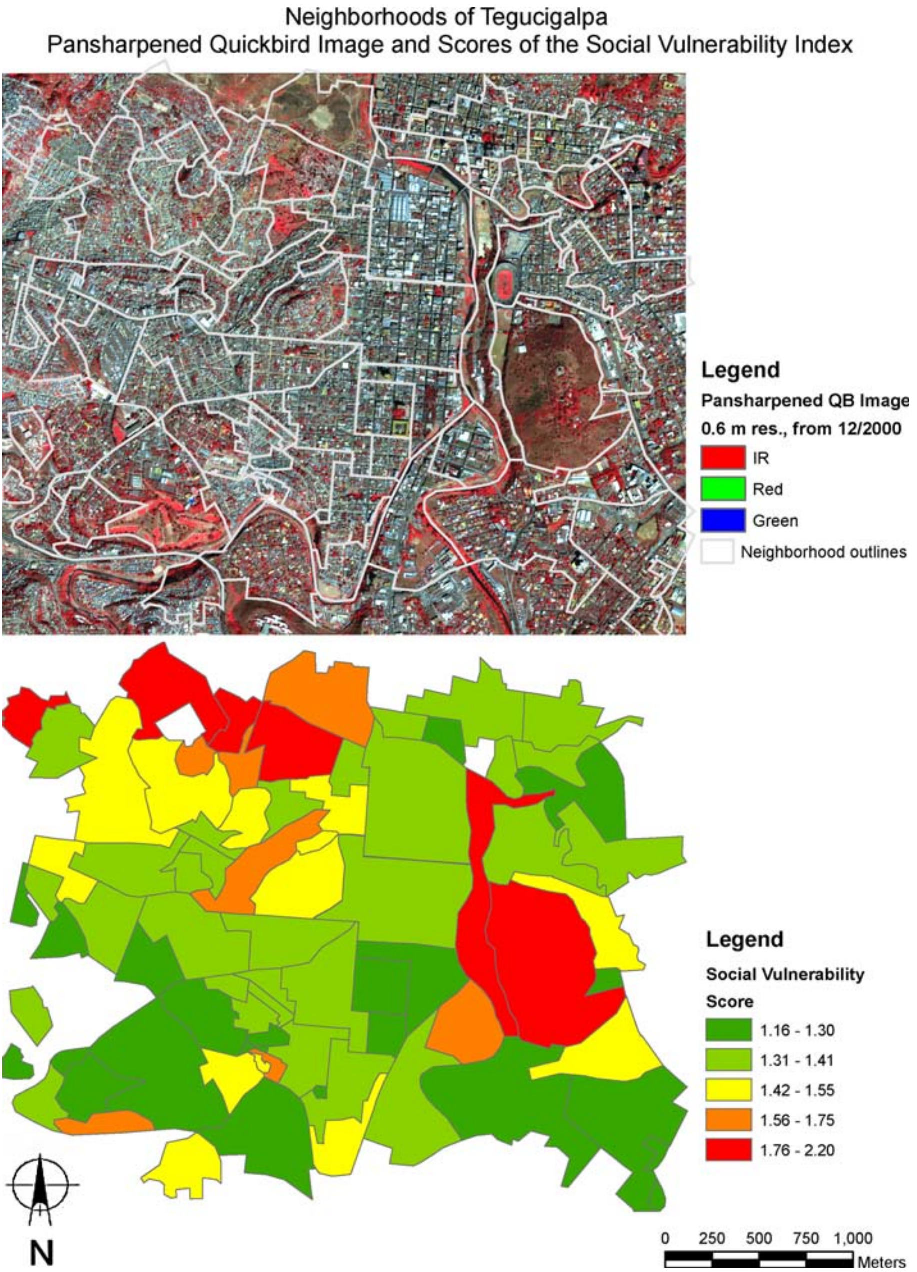

Fig. 4 Scores from the social vulnerability index per neighborhood (bottom) with the pansharpened Quickbird image as reference (top)

separated into paved and barren roads, yielding the fraction of paved roads within the total road network in each neighbourhood. A high proportion of paved roads corresponds to a high development of the neighbourhood.

Building types and state have been identified previously as physical expressions of SV (Cutter et al. 2003; Rashed and Weeks 2003b). Hence in imagery, largely restricted to a vertical perspective, the roof construction material may be a useful proxy for the socio-economic status of the building occupants. Due to the lack of ground data on actual roof materials, it was tested whether different materials that can be distinguished in the satellite data have a statistical potential to explain SV variation. Seven different roof types were classified from the Quickbird image, and the proportion of each roof type calculated compared to the total area covered by buildings.

The available service infrastructures (commercial centres, transport infrastructure, institutional or governmental buildings, gas stations, universities) were digitized from existing city maps (Table 1) and quantified for each neighbourhood as another indicator for development. In case such infrastructure information is not available for a given study area, visual image analysis or tools such as Google Earth could be used to identify large commercial areas or transport hubs such as bus or train stations.

To describe the topographic location, the slope position was calculated from the DTM, to which each image object was then associated. Using membership functions, only the built-up areas were masked and combined with the slope information. Twelve slope classes in 5° intervals, from 0° to 60°, were delineated. As another supporting proxy variable, all buildings in a flood or landslide hazard zone (delineation based on existing USGS hazard maps prepared in 2002) were masked out, and the percentage compared to all buildings in the neighbourhood calculated.

Building heights were delineated from the lidar data set that covers only a part of the study area (Table 2). Using this supporting proxy variable, the commercial development was characterized. In Tegucigalpa, high buildings (>7 stories) can to a large extent be associated with commercial or industrial development, which in turn is regarded as an indicator for low SV values.

Lastly, three possible distances to service infrastructure and lifelines (<100, 100–250, >250 m) were defined using membership functions, relating the position of each building to those features.

A total of 47 supporting proxy variables (Table 3) were delineated from the digital data sets to describe the three original indicators for SV (first column in Table 3). While delineating proxy variables, information about the environment was derived from different data sources as shown in Table 1. By using membership functions and fuzzy rule sets, each classified image object was characterized according to its (i) slope, (ii) distance to hazard zone and (iii) distance to service infrastructure. In addition, spatial metrics (Herold et al. 2003; Rashed and Weeks 2003b) were calculated from the classification-based land use/land cover information to describe the settlement characteristics for each administrative neighbourhood.

5 Validation of the derived indicators

5.1 Delineation of a Social Vulnerability Index (SVI)

After the extraction of the 47 proxies, their relevance as predictors of SV was tested. In a previous study, SV was calculated based on spatial metrics and compared with values derived from multi-criteria GIS analysis (Rashed and Weeks 2003b). Here, using a traditional method for comparison, a reference SV map on a neighbourhood level in Tegucigalpa based on the 2000 census data and the method used by Cutter et al. (2003)

was calculated. Seven main variables were available: (i) gender, (ii) literacy, (iii) roof material, (iv) wall material, (v) water availability, (vi) waste disposal and (vii) building type.

These variables differ from those employed in image analysis. This complicates a direct comparison of the results but also reflects the reality of the different methods with which SV is being assessed. Rashed and Weeks (2003b) faced a similar problem when they used an index of wealth (based on census data) and an index of vulnerability (based on HAZUS seismic risk simulations) to assess the explanatory potential of image-based SV proxies.

The alternatives for each variable (e.g. male and female for gender) were ranked according to their impact on SV based on previous research (Ranganath 2000; Cutter et al. 2003; Haki et al. 2004) and field observations (Angel et al. 2004). Pairwise comparison (Saaty 1980) was used to assign weights to all alternatives based on their ranking. A Social Vulnerability Index (SVI) adapted from Haki et al. (2004) was then applied to calculate the SV per neighbourhood based on the census data:

$$\mathrm{SV} = \sum_{i=1}^{m} v_i q_i \tag{2}$$

where SV is the vulnerability score for each neighbourhood, v_i is the weight derived from the pairwise comparison for each variable (values ranging from 0 to 1), and q_i is the relative frequency of the variable per neighbourhood (values ranging from 0 to 1). Calculated values for each neighbourhood are shown in Fig. 4 (bottom). A similar additive calculation was also used by Cutter et al. (2003), whereas Wu et al. (2002) normalized SV values to range between 0 and 1. This presents a conceptual challenge for quantitative risk assessment. While physical or economic vulnerability characterize a clearly quantifiable degree of loss, a SV concept that links to a person's ability to anticipate, cope with, resist to and recover from the impact of a hazardous event (Wisner et al. 2004) faces challenges such as scaling. Indeed, Adger and Kelly (1999) and Smit and Pilifosova (2003) focus on understanding functional relationships rather that calculating absolute SV values. For Rashed and Weeks (2003a), an assessment of SV in absolute terms is not possible, as it is continuously modified and varies over space and time. Hence, our principal aim is to identify variables that help explain how SV is generated, and it is concurred with Clark et al. (1998) for whom the main purpose of vulnerability maps is the ability to identify threatened populations and areas on which to focus limited resources.

5.2 Quantitative spatial analysis

A two-step procedure to identify the significant variables to explain SV was used. First, a stepwise regression model was used, based on ordinary least squares, to select those variables out of the set of 47 proxy variables that significantly contribute to explaining the vulnerability score SV from the SVI (Draper and Smith 1981; Rashed and Weeks 2003b; Jain 2005). In a stepwise regression, the variables are entered and/or removed successively and thus accepted for inclusion if a tolerance threshold p_{IN} is exceeded for entrance and a p_{EX} is no longer exceeded for exclusion. After testing various values for p_{IN}, it was decided to use a p_{IN}-value of 0.15. These values were large enough to allow also entering of less strongly related explanatory variables into the regression model, hence remaining on the safe side. A somewhat lower p_{EX} value of 0.1 ensured that no endless iterations occurred.

The second step used spatial regression to estimate values of the coefficients on the comprehensive set of explanatory variables thus obtained (Cressie 1991). The neighbourhood structure was identified and a simultaneous autoregression (SAR) spatial covariance family was applied.

The results of the analysis are given in Table 4. The model explained almost 60% of the changes in SV ($R^2 = 0.595$). The following can be noticed:

- A high *proportion of built-up areas* and of *buildings on gentle slopes* corresponds to low SV.
- A high *proportion of buildings on medium slopes, buildings exposed to landslide hazard* and the *abundance of two specific roof types* corresponds to high SV values.
- A high *amount of infrastructure* corresponds to high SV, although at low significance. This is somewhat surprising and most likely this variable provides a correction on the other variables, compensating some of the variation in the variables with a higher significance, such as *buildings at landslide hazard*. It may also be the case that the amount of service infrastructure and lifelines is higher around buildings exposed to landslide hazard because of planning considerations by the city developers in the past.
- No significant influence was found for the selected *texture measures,* the *amount of buildings at flood risk* and the *distance to infrastructure* (e.g. lifelines).
- Absolute sizes of the effects can be large (18.477 for *slope9* and −157.1 for *slope12*), but these values correspond to very low fractions occurring in the study area (0.00026 for *slope12* and 0.0026 for *slope9*).

The variables *impervious* and *slope11* were entered at intermediate stages, but after inclusion of *built3* and *propbuilt*, the variable *impervious* was removed from the model, as it did not significantly contribute to explaining the variation in SV. Similarly, *slope11* was removed after inclusion of *slope9* and *slope12*. Also the model was compared thus selected with models obtained with p_{IN}-values equal to 0.05, 0.1 and 0.2, but the original model was found to be the best interpretable one.

For the lidar data, the *proportion of buildings with more than 6 floors* (*stor7*), interpreted as an indicator for commercial development, was found to have a significant explanatory value ($R^2 = 0.451$), with higher proportions indicating lower SV.

Although the regression results are largely plausible and confirm the hypothesis that image-derived parameters can provide information on the distribution of SV, it also signals a potential problem. Table 4 shows that the higher the *proportion of buildings on medium slopes* (*slope9*) the higher the SV, with an opposite effect for *buildings on very steep slopes* (*slope12*).

The likely reason is the occurrence of many zeros in the dataset, in particular when the fraction of buildings on steep slopes is considered. These fractions are zero in many neighbourhoods, reflecting the low number of steep slopes in the study area. In the analysis this has led to an anomaly where the non-zero observation for these classes has a disproportionately large effect.

Thus, it may be preferable to aggregate such variables into fewer classes.

6 Discussion

The frequent lack of suitable data, as well as conceptual difficulties, explain why many studies do not incorporate SV assessment as a critical aspect of a comprehensive risk assessment. Existing methods either use data with limited suitability and availability (census data) or rely on detailed house-to-house surveys that are insightful but preclude wider and more frequent use. The goal of this study was to test the utility of indicators of

Table 4 Results from the stepwise regression model for the explanation of the vulnerability scores VPC (pos., positive effect; neg., negative effect)

Step	Variable entered	Variable removed	No. of variables	Partial R^2	Model R^2	F-value	Pr > F (P-value)	Estimated parameter
1	Proportion of houses on slopes between 5° and 10° (*slope2*)		1	0.2333	0.2333	23.44	<0.0001	−0.8623
2	Proportion of impervious surface (*Impervious*)		2	0.1174	0.3507	13.74	0.0004	–
3	No. of buildings at landslide risk (*lshaz*)		3	0.0568	0.4075	7.18	0.0090	0.4335
4	Proportion of roof type 3 (*built3*)		4	0.0509	0.4584	6.96	0.0102	0.5740
5	Number of infrastructure in neighbourhood (*numberIS*)		5	0.0393	0.4977	5.71	0.0195	0.0378
6	Proportion of houses on slopes between 50° and 55° (*slope11*)		6	0.0161	0.5138	2.39	0.1269	–
7	Proportion of built-up area (*propbuilt*)		7	0.0175	0.5313	2.65	0.1077	−0.8550
8		*Impervious*	6	0.0025	0.5288	0.39	0.5368	–
9	Proportion of houses on slopes between 40° and 45° (*slope9*)		7	0.0228	0.5515	3.60	0.0617	18.477
10	Proportion of houses on slopes between 55° and 60° (*slope12*)		8	0.0321	0.5836	5.39	0.0231	−157.1
11		*slope11*	7	0.0058	0.5778	0.97	0.3276	–
12	Proportion of roof type 6 (*built6*)		8	0.0175	0.5953	3.02	0.0864	0.417
	for nDSM[a]							
1	Proportion of buildings with more than 6 floors (*stor7*)		1	0.4509	0.4509	13.14	0.0023	−9.155

[a] nDSM, normalized digital surface model

SV from high resolution images and other spatial data using OOA. Proxy variables, i.e. variables that translate and express the not-directly observable concept of SV, had to be defined and identified, and their explanatory capacity had to be assessed. The 47 proxy variables delineated were tested in a stepwise regression analysis and could explain almost 60% of the variation of a reference SVI calculated from census data with conventional methods (Wu et al. 2002; Cutter et al. 2003).

The initial land cover/use classification of the pansharpened Quickbird image using OOA is a critical basis for the delineation of spatial metrics and the advanced land use classes that incorporate GIS data (e.g. hazard zones) and the DTM (Table 3). Based on this information, contextual analysis allowed suitable proxy variables to be defined that describe non-physical indicators of SV. In this study the high spatial resolution was more valuable than high spectral resolution, as many relevant details, such as single houses, could be identified. The incorporation of lidar data was very useful to extract building heights. Since such data are rather cost-intense, they might not be always available. Nevertheless, building heights can also be extracted from stereo-images or orthophotos (Fraser et al. 2002). A higher spectral resolution might have allowed a more detailed assessment of construction and roof materials. Indeed, Rashed and Weeks (2003b) based their land cover assessment for SV analysis on Landsat TM data.

The proxy variables defined described the non-physical concept of SV to a substantial degree, though it is clear that SV assessment also comprises a range of indicators that have no physical expression and thus cannot be delineated from image data, e.g. gender, age, knowledge about the hazard and individual disaster preparedness (Cutter et al. 2003). Although no comprehensive assessment of SV is feasible with image data alone, it can help overcome the low spatial detail of census-based SV assessment. In Cutter et al.'s approach, the spatial resolution is limited to the 3,141 US counties (with approximately 100,000 people in one census tract). Rashed and Weeks (2003b), who also used US census data, also concluded that both the social and the physical aspects of SV need to be understood and that thus census data alone are not sufficient. Finally, it has to be stressed that also SV is hazard-dependent. For example, while meteorological hazards such as heatwaves challenge an individual's health coping capacities (Nakai et al. 1999), floods pose a more immediate physical threat to younger and shorter people. In the SV analysis, weights have to be assigned that correspond to such individual characteristics, leading to particular challenges when multi-hazard vulnerability is to be assessed.

The method presented here can also help overcome high cost and limited spatial coverage of ground surveys. Figure 5 illustrates the cost-benefit concept of an integrated approach. The use of satellite data (solid lines) is efficient compared to house-to-house surveys, comparatively easy to repeat and relatively low in cost per mapping unit, but by itself not detailed enough for a comprehensive assessment of SV. Most detailed but also most expensive and time-consuming are house-to-house surveys, while census data are most efficient but least detailed (both in dashed line). In general, the higher the level of detail, the higher the costs and the higher the time input required for data processing. The gap between the dashed and the solid line shows the trade-off between costs, efficiency and the level of detail. The level of detail is a relative measure compared to the alternative method. The width of the cost-benefit area is mainly dependent on the accepted trade-off at the considered scale. In general, the higher the level of detail required, the higher the costs and the lower the efficiency.

Additionally, image data are available more frequently than census or ground information and the methodology is generic, thus can be applied in other areas if adapted to the data availability and scale of the area of interest, while also allowing the dynamics of SV to

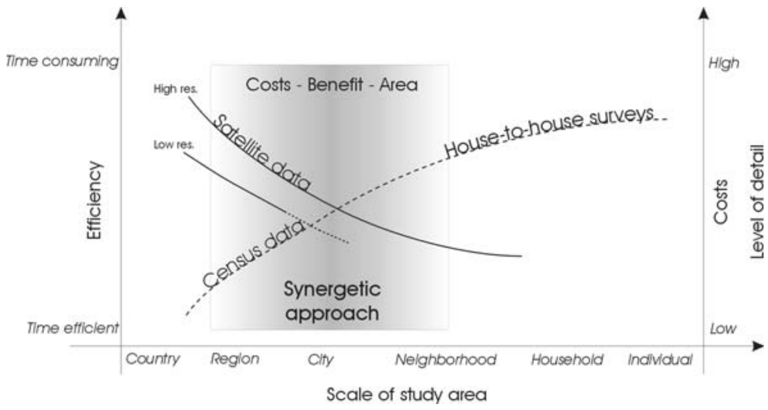

Fig. 5 Cost-benefit area of an integrated approach for the assessment of social vulnerability implementing both traditional field surveys and remote sensing and GIS technology

be captured. For the definition of proxy variables, local knowledge about the study area is inevitable.

Although the proxies are generic to a large extent, they have to be adapted and evaluated to suit the specific situation. Most important is that the key factors that drive SV in the specific region are recognized and translated into appropriate variables. However, exactly such adaptation is also needed for alternative SV assessment methods. Census-based approaches have to be modified depending on the variables available, while community-based work, be it based on focus groups or questionnaires, has to adapt to the local setting, as well as hazards present.

It is argued that the optimal approach for SV assessment is a combination of both traditional methods (analysis of census data and community-based surveys) and new geo-informatics-based methodologies (OOA of high-resolution satellite and other spatial data).

The potential of OOA for the delineation of proxy variables has also yet to be fully realized. The combination of different data sources and object information offers a variety of possibilities to describe single segments or a group of adjacent segments (e.g. neighbourhoods). The better the understanding of SV, the better the resulting proxy variables. That means that the results and assessment methods based on remote sensing data can be improved if more extensive input is given from social scientists that work on a definition and indicators of SV. The increasingly rich conceptual basis for vulnerability assessment emerging from previously disparate research fields (Eakin and Luers 2006) is particular encouraging. Similarly, the better the relation between SV indicators and their physical expression in urban morphology is understood, the more suitable and better adapted to non-visible concepts the description of proxy variables can be.

Even if only data with medium spatial resolution are available, some relevant indicators, such as settlement extent and texture measures for the characterization of the settlement, can be delineated. Recent studies on satellite data interchangeability for urban risk assessment showed that also medium resolution data, e.g. from Landsat TM, can be used to delineate land use classes such as built-up areas and vegetation to a sufficient degree (Rashed and Weeks 2003b; Shamaoma et al. 2006). Those were also the classes that proved to be important for this study, and thus while high spatial resolution improves the accuracy, medium resolution data can also be applied. However, this emphasizes also that more than one method exists to calculate SV.

7 Conclusions

In this article it could be shown that OOA comprising the evaluation of contextual information and the analysis of image segments on several scales is a valuable tool for the delineation of a variety of proxy variables that can describe non-physical indicators of SV that are not directly mappable.

These proxy variables were derived from air- and spaceborne imagery as well as GIS data and successfully used to describe those indicators of SV that relate to the socio-economic status of a household and to settlement characteristics of a neighbourhood. It can be argued that, when used in conjunction with limited ground-based data and improved spatial extrapolation techniques, it constitutes an optimized and more economical approach. Thus, the methodology presented here can be considered as a significant contribution to disaster management, especially for rapidly changing but data scarce areas.

Acknowledgements We would like to thank Micah Perlin from Princeton University for providing GIS-Data, Guillermo Suazo from PMDN for providing the DTM and census data and Kunda MM Rao from NRSA for making available the Indian ResourceSat P-6 image.

References

Adger WN, Kelly PM (1999) Social vulnerability to climate change and the architecture of entitlements. Mitigation Adapt Strat Glob Change 4(3–4):253–266

Angel S, Bartley K, Derr M, Malur A, Mejia J, Nuka P, Perlin M, Sahai S, Torrens M, Vargas M (2004) Rapid urbanization in Tegucigalpa, Honduras. Preparing for the doubling of the city's population in the next twenty-five years. Report from Woodrow Wilson School of Public and International Affairs, Princeton University, 74 pp

Allen KM (2006) Community-based disaster preparedness and climate adaptation: local capacity-building in the Philippines. Disasters 30:81–101. doi:10.1111/j.1467-9523.2006.00308.x

Arciniegas G, Bijker W, Kerle N, Tolpekin V (2007) Coherence- and amplitude-based analysis of seismogenic damage in Bam, Iran, using Envisat ASAR data. IEEE Trans Geosci Remote Sens 45:1571–1581. doi:10.1109/TGRS.2006.883149

Baatz M, Benz U, Dehghani S, Heynen M, Höltje A, Hofmann P, Lingenfelder I, Mimler M, Sohlbach M, Weber M, Willhauck G (2004) eCognition user guide 4. Munich

Bacon C, Mastin L, Scott K, Nathenson M (1997) Volcano and earthquake hazards in the Crater Lake region, Oregon. U.S. Geological Survey Open-File Report 97-487

Balz T, Haala N (2003) SAR-based 3D-reconstruction of complex urban environments. Int Arch Photogramm Remote Sens 34:181–185

Birkmann J (2005) Measuring vulnerability. Report on the 1st meeting of the expert working group "Measuring Vulnerability" of the United Nations University Institute for Environment and Human Security (UNU-EHS), Bonn

Blaschke T, Strobl J (2001) What's wrong with pixels? Some recent developments interfacing remote sensing and GIS. GIS 6:12–17

Briguglio L (2003) The vulnerability index and small island developing states: a review of conceptual and methodological issues. Department of Economics, University of Malta, Msida

Cardona OD (2003) Indicators for disaster risk management. First expert meeting on disaster risk conceptualization and indicator modelling. Manizales, March 2003

Clark GE, Moser S, Ratick S, Dow K, Meyer WB, Emani S, Jin W, Kasperson JX, Kasperson RE, Schwarz HE (1998) Assessing the vulnerability of coastal communities to extreme storms: the case of Revere, MA, USA. Mitigation Adapt Strat Glob Change 3(1):59–82

CINDI (1998) Central America: Hurricane Mitch OFDA-12: 12-Nov-98. USAID/OFDA Hurricane Mitch Fact Sheet 12

Coburn AW, Spence RJS, Pomonis A (1994) A vulnerability and risk assessment, 2nd edn. United Nations Development Programme (UNPD)

Cressie NAC (1991) Statistics for spatial data. Wiley, New York

Cutter SL, Boruff BJ, Shirley WL (2003) Social vulnerability to environmental hazards. Soc Sci Q 82:242–260. doi:10.1111/1540-6237.8402002

Dash J, Steinle E, Singh RP, Baehr HP (2004) Automatic building extraction from laser scanning data: an input tool for disaster management. Adv Space Res 33:317–322. doi:10.1016/S0273-1177(03)00482-4

Davidson C (2006) Was 2005 the year of natural disasters? Bull World Health Organ 84:4–8

Draper NR, Smith H (1981) Applied regression analysis. In: Bradley RA, Hunter JS, Kendall DG, Watson GS (eds) Wiley series in probability and mathematical statistics. Wiley, New York

Dwyer A, Zoppou C, Nielsen O, Day S, Roberts S (2004) Quantifying social vulnerability: a methodology for identifying those at risk to natural hazards. Geoscience Australia

Eakin H, Luers AL (2006) Assessing the vulnerability of social-environmental systems. Annu Rev Environ Resour 31:365–394. doi:10.1146/annurev.energy.30.050504.144352

Emdad Haque C, Etkin D (2007) People and community as constituent parts of hazards: the significance of societal dimensions in hazards analysis. Nat Hazards 41:271–282. doi:10.1007/s11069-006-9035-8

Espindola G, Camara G, Reis I, Bins L, Monteiro A (2006) Parameter selection for region-growing image segmentation algorithms using spatial autocorrelation. Int J Remote Sens 27:3035–3040. doi:10.1080/01431160600617194

Flint CG, Luloff AE (2005) Natural resource-based communities, risk, and disaster: an intersection of theories. Soc Nat Resour 18:399–412. doi:10.1080/08941920590924747

Fraser C, Baltsavias E, Gruen A (2002) Processing of Ikonos images for submetre 3D positioning and building extraction. ISPRS J Photogramm Remote Sens 56:177–194. doi:10.1016/S0924-2716(02)00045-X

Gao Y, Kerle N, Mas JF, Navarrete A, Niemeyer I (2007) Optimised image segmentation and its effect on classification accuracy, Spatial Data Quality 2007, Enschede, 4 pp

Giardino M, Mondino EB, Perotti L (2005) Geomatics application for geological and geomorphological mapping and landslide hazard evaluation: case studies in the Italian NW-Alps. In: 31st International symposium on remote sensing of environment, Saint Petersburg

Haki Z, Akyuerek Z, Duezguen S (2004) Assessment of social vulnerability using Geographic Information Systems: Pendik, Istanbul case study. In: 7th AGILE conference on geographic information science, Heraklion

Herold M, Clarke K (2007) Remote sensing derived mapping to support urban growth theory. In: Weng Q, Quattrochi DA (eds) Urban remote sensing. Taylor & Francis, 500 pp

Herold M, Liu X, Clarke KC (2003) Spatial metrics and image texture for mapping urban land use. Photogramm Eng Remote Sens 69:991–1001

Hirschmugl M, Gallaun H, Perko R, Schardt M (2005) “Pansharpening” - Methoden für digitale, sehr hochauflösende Fernerkundungsdaten. In: 17. AGIT symposium, Salzburg

Iverson R, Schilling S, Vallance J (1998) Objective delineation of lahar-inundation hazard zones. Geol Soc Am Bull 110:972–984. doi:10.1130/0016-7606(1998)110<0972:ODOLIH>2.3.CO;2

Jain S (2005) System evolution using high resolution satellite data for urban regimes. PhD thesis, Department of Architecture and Planning, Indian Institute of Technology Roorkee

Kerle N (2002) Volume estimation of the 1998 flank collapse at Casita volcano, Nicaragua: a comparison of photogrammetric and conventional techniques. Earth Surf Process Landf 27:759–772. doi:10.1002/esp. 351

Lawrence W, Imhoff M, Kerle N, Stutzer D (2002) Quantifying urban land use and impact on soils in Egypt using diurnal satellite imagery of the Earth surface. Int J Remote Sens 23:3921–3937. doi:10.1080/01431160110115951

Lee S, Choi J, Min K (2004) Probabilistic landslide hazard mapping using GIS and remote sensing data at Boun, Korea. Int J Remote Sens 25:2037–2052. doi:10.1080/01431160310001618734

Müller M, Segl K, Heiden U, Kaufmann H (2006) Potential of high-resolution satellite data in the context of vulnerability of buildings. Nat Hazards 38:247–258. doi:10.1007/s11069-005-8637-x

Myint SW (2007) Urban mapping with geospatial algorithms. In: Weng Q, Quattrochi DA (eds) Urban remote sensing. Taylor & Francis, 500 pp

Nakai S, Itoh T, Morimoto T (1999) Deaths from heat-stroke in Japan: 1968–1994. Int J Biometeorol 43:124–127. doi:10.1007/s004840050127

O’Hare G, Rivas S (2005) The landslide hazard and human vulnerability in La Paz City, Bolivia. Geogr J 171:239–258. doi:10.1111/j.1475-4959.2005.00163.x

Ramsey M, Flynn L (2004) Strategies, insights, and the recent advances in volcanic monitoring and mapping with the data from NASA’s Earth Observing System. J Volcanol Geotherm Res 135:1–11. doi:10.1016/j.jvolgeores.2003.12.015

Ranganath P (2000) Mitigation and the consequences of international aid in post disaster reconstruction. McGill University and University of Colorado, Natural Hazards Research Working Paper 103

Rashed T, Weeks J (2003a) Assessing vulnerability to earthquake hazards through spatial multicriteria analysis of urban areas. Int J Geogr Inf Sci 17:547–576. doi:10.1080/1365881031000114071
Rashed T, Weeks J (2003b) Exploring the spatial association between measures from satellite imagery and patterns of urban vulnerability to earthquake hazards. Int Arch Photogramm Remote Sens Spat Inf Sci XXXIV 7(W9):144–152
Ridd MK (1995) Exploring a V-I-S (vegetation-impervious surface-soil) model for urban ecosystems analysis through remote sensing: comparative anatomy for cities. Int J Remote Sens 16:2165–2185. doi:10.1080/01431169508954549
Saaty TL (1980) The analytic hierarchy process. McGraw-Hill International Book Company, New York
Shamaoma H, Kerle N, Alkema D (2006) Extraction of flood-modelling related base-data from multi-source remote sensing imagery. In: ISPRS mid-term symposium 2006 remote sensing: from pixels to processes, Enschede, 8–11 May 2006
Smit B, Pilifosova O (2003) From adaptation to adaptive capacity and vulnerability reduction. In: Huq S, Smith J, Klein RTJ (eds) Enhancing the capacity of developing countries to adapt to climate change. Imperial College Press, London
Stilla U, Sörgel U, Thönnessen U (2003) Potential and limits of InSAR data for building reconstruction in built up-areas. ISPRS J Photogramm Remote Sens 58:113–123. doi:10.1016/S0924-2716(03)00021-2
Tralli DM, Blom RG, Zlotnicki V, Donnellan A, Evans DL (2005) Satellite remote sensing of an earthquake, volcano, flood, landslide and coastal inundation hazards. ISPRS J Photogramm Remote Sens 59:185–198. doi:10.1016/j.isprsjprs.2005.02.002
Tuceryan M, Jain A (1998) Texture analysis. In: Chen C, Pau L, Wang P (eds) The handbook of pattern recognition and computer vision, 2nd edn. World Scientific Publishing Co., pp 207–248
UNDP (2005) Human development report. International cooperation at a crossroads. Aid, trade and security in an unequal world, New York
van Westen CJ, Kumar Piya B, Guragain J (2005) Geoinformation for urban risk assessment in developing countries; the SLARIM project. In: 1st International symposium on geo-information for disaster management, Delft
Villagrán de León JC (2006) Vulnerability. A conceptual and methodological review. UNU-EHS, Bonn
Vosselman G, Gorte BGH, Sithole G, Rabbani T (2004) Recognising structure in laser scanner point clouds. Int Arch Photogramm Remote Sens Spat Inf Sci 36(8/W2):33–38
Wisner B, Blaikie P, Cannon T, Davis I (2004) At risk. Natural hazards, people's vulnerability and disasters. Routledge, London
Wu SY, Yarnal B, Fisher A (2002) Vulnerability of coastal communities to sea-level rise: a case study of Cape May County, New Jersey, USA. Climate Res 22:255–270
Zhang Y, Maxwell T (2006) A fuzzy logic approach to supervised segmentation for object-oriented classification. In: ASPRS 2006 annual conference, Reno